Golli Protein Negatively Regulates Store Depletion-Induced Calcium Influx in T Cells

Ji-Ming Feng,[1,*] Yanhong K. Hu,[1] Lai-Hua Xie,[2]
Christopher S. Colwell,[1] Xuesi M. Shao,[3]
Xiao-Ping Sun,[4] Boming Chen,[4] Hezhen Tang,[1]
and Anthony T. Campagnoni[1,*]
[1] Semel Institute of Neuroscience and Human Behavior
[2] Department of Cardiology
[3] Department of Neurobiology
[4] Department of Physiology
UCLA Geffen School of Medicine
635 Charles Young Drive
Los Angeles, California 90095

Summary

Calcium influx is crucial for T cell activation and differentiation. The detailed regulation of this process remains unclear. We report here that golli protein, an alternatively spliced product of the myelin basic protein gene, plays a critical role in regulating calcium influx in T cells. Golli-deficient T cells were hyperproliferative and showed enhanced calcium entry upon T cell receptor stimulation. We further found that golli regulates calcium influx in T cells through the inhibition of the store depletion-induced calcium influx. Mutation of the myristoylation site on golli disrupted its association with the plasma membrane and reversed its inhibitory action on Ca^{2+} influx, indicating that membrane association of golli was essential for its inhibitory action. These results indicate that golli functions in a unique way to regulate T cell activation through a mechanism involving the modulation of the calcium homeostasis.

Introduction

Elevation of the cytosolic calcium (Ca^{2+}) concentration is critical for T cell activation, proliferation, and differentiation (Lewis, 2001; Feske et al., 2000, 2001, 2003). Ca^{2+} elevation in activated T cells occurs primarily through capacitative calcium entry (CCE) via store-operated Ca^{2+} channels (SOCCs). CCE is activated by depletion of Ca^{2+} from intracellular Ca^{2+} stores (e.g., the endoplasmic reticulum [ER]). Engagement of the T cell receptor (TCR) activates phospholipase Cγ1 (PLCγ1), which subsequently hydrolyzes membrane phospholipids to produce the second messenger, inositol 1,4,5-triphosphate (IP3). IP3 interacts with IP3 receptors on the ER that serve to release luminal-stored Ca^{2+} and generate a "depleted" status of the ER stores (Putney 1990; Berridge 1993; Clapham, 1995; Parekh and Penner, 1997; Putney and McKay, 1999; Putney et al., 2001; Venkatachalam et al., 2002). The decline of Ca^{2+} levels within the lumen of the ER transmits an unidentified signal to the plasma membrane, resulting in the opening of SOCCs, which, in turn, permits external Ca^{2+} to enter the cells. This Ca^{2+}

entry sustains elevated cytosolic Ca^{2+} concentrations and provides a means of replenishing intracellular Ca^{2+} stores. The mechanism by which ER Ca^{2+} store depletion is coupled to external Ca^{2+} entry is not clear. In this study, we investigated the role that a golli protein, a product of the myelin basic protein (mbp) gene, plays in the regulation of store depletion-induced Ca^{2+} entry into T cells.

The mbp gene encodes two families of structurally related proteins generated through alternative splicing (i.e., classic MBPs and golli-MBPs, as shown in Figure S1; see the Supplemental Data available with this article online). Classic MBPs serve as major structural protein constituents of myelin in the central and peripheral nervous systems. The second family of proteins encoded by the mbp gene consists of the golli proteins, whose function is less understood. The major golli products contain the MBP1-56 sequence in their C-terminal halves, but they differ from the classic MBPs in that they contain, at their N termini, a 133 amino acid (aa) sequence that is unique to the golli proteins. This sequence is encoded by five exons upstream of the classic MBP transcription start site (Campagnoni et al., 1993; Campagnoni and Skoff, 2001). Unlike classic MBPs, which are exclusively expressed in myelin-forming cells in the nervous system, golli mRNAs are expressed in the thymus and other immune organs at amounts comparable to those in the brain. In thymus, golli proteins are primarily expressed in developing thymocytes, and the levels of golli expression in thymocytes vary with their differentiation state (Feng et al., 2000). Relative to immature CD4$^+$CD8$^+$ double positive (DP) thymocytes, mature CD4$^+$ or CD8$^+$ single positive (SP) thymocytes express higher levels of golli (Feng et al., 2000). In spleen, T cells express substantially higher amounts of golli than B cells. In vitro transfection of golli into Jurkat T cells can inhibit IL-2 gene transcription upon TCR engagement (Feng et al., 2004). Although golli possesses several protein kinase C (PKC) phosphorylation sites within its MBP domain, the inhibitory function of golli has been shown to be independent of its PKC phosphorylation (Feng et al., 2004). Mutagenesis studies (Feng et al., 2004) showed that the inhibitory function resides in the golli domain alone (133 aa). The exact role of golli in T cell signal transduction is unknown. To investigate further how golli regulates T cell function, we generated golli-deficient mice and found that the ablation of golli in T cells results in hyperproliferation, consistent with our previous finding that golli serves as a negative regulator of T cell activation. However, unlike other negative regulators of T cell activation, such as Cbl-b (E3 ubiquitin ligase) and DGK (diacylglycerol kinase), which act on the kinase arm of TCR signaling, we found that golli uniquely acts on TCR signaling by inhibiting store depletion-induced Ca^{2+} entry.

Results

Golli Proteins Are Located in T Cell-Rich Areas of the Spleen and Can Associate with the Plasma Membrane of the T Cell

In the thymus, golli is expressed primarily in thymocytes, and the levels of golli expression in thymocytes change

*Correspondence: jfeng@mednet.ucla.edu (J.-M.F.); acampagnoni@mednet.ucla.edu (A.T.C.)

with differentiation state (Feng et al., 2000). In spleen, golli immunoreactivity is located primarily in the periarteriolar lymphoid sheath (PALS), a T cell-enriched region (Figure 1A). Flow cytometry studies have confirmed that T cells expressed markedly higher amounts of golli than B cells in peripheral lymphoid organs (Feng et al., 2004).

We next examined the subcellular distribution of golli in T cells. Most golli proteins are present in the cytosol (Figure 1B). We have shown the two major alternatively spliced golli isoforms, BG21 and J37, to have an M_r of 31 kDa and 35 kDa, respectively, in SDS-PAGE (Landry et al., 1996). In immune tissues and cells, golli BG21 is the predominant (virtually the only) isoform expressed (Feng et al., 2004). Based on the molecular weights of the golli products (shown in Figure 1B), it was likely that the smaller band (M_r of ~25 kDa) was a cleavage product of the larger band (M_r of ~30–31 kDa), which ran with an M_r corresponding to that of BG21. We confirmed this by solely transfecting BG21 cDNA into Jurkat T cells and performing an immunoblot on the lysates (Figure 1C). The immunoblot showed two bands with identical molecular weights to those seen in Figure 1B in the primary T cells, suggesting that, in T cells, the golli BG21 undergoes cleavage to a smaller product. A fraction of "cleaved" golli protein was observed to be associated constitutively with the plasma membrane of primary T cells (Figure 1B), and, in Jurkat T cells, transfected golli, tagged with green fluorescence protein (GFP), was found by confocal microscopy to distribute on the plasma membrane and in multivesicular aggregates in the cytoplasm (Figure 1D). The membrane association of golli in primary T cells was enhanced (Figure 1B) by TCR engagement (e.g., after 10 min of stimulation with anti-CD3). Unlike with Lck (p56[Lck], lymphocyte-specific protein tyrosine kinase), a fraction of which was shown to be redistributed to the cytoskeleton after 30 min of stimulation, there was no detectable golli found in the cytoskeleton of either stimulated or unstimulated T cells (Figure 1B). Thus, the data indicate that golli is moved within the cells, possibly by transport vesicles, to the plasma membrane. It also suggests that, in T cells, golli BG21 undergoes cleavage to a smaller form that can associate with the cell membrane.

Normal Thymocyte Development, but Abnormal Accumulation of Peripheral T Cells, in Golli-Deficient Mice

In previous work, we found that overexpression of golli BG21 in Jurkat T cells resulted in reduced IL-2 gene transcription, indicating that golli protein could function as a negative regulator of T cell activation (Feng et al., 2004). To explore this further, we generated golli-deficient mice by ablating exon 2 of the *mbp* gene (Voskuhl et al., 2003; Jacobs et al., 2005), which includes the translation initiation site for the golli proteins. In these mice, the amounts of classic MBPs in brain were not affected by the golli ablation. Ablation of the golli gene products was confirmed by FACS analysis, showing no golli-specific staining in golli-deficient thymocytes (Figure 2A, left panel), and immunoblot analysis, showing the absence of a golli protein band in the lysates from golli-deficient lymphoid cells (Figure 2A, right panel). The mutant mice are maintained on a mixed
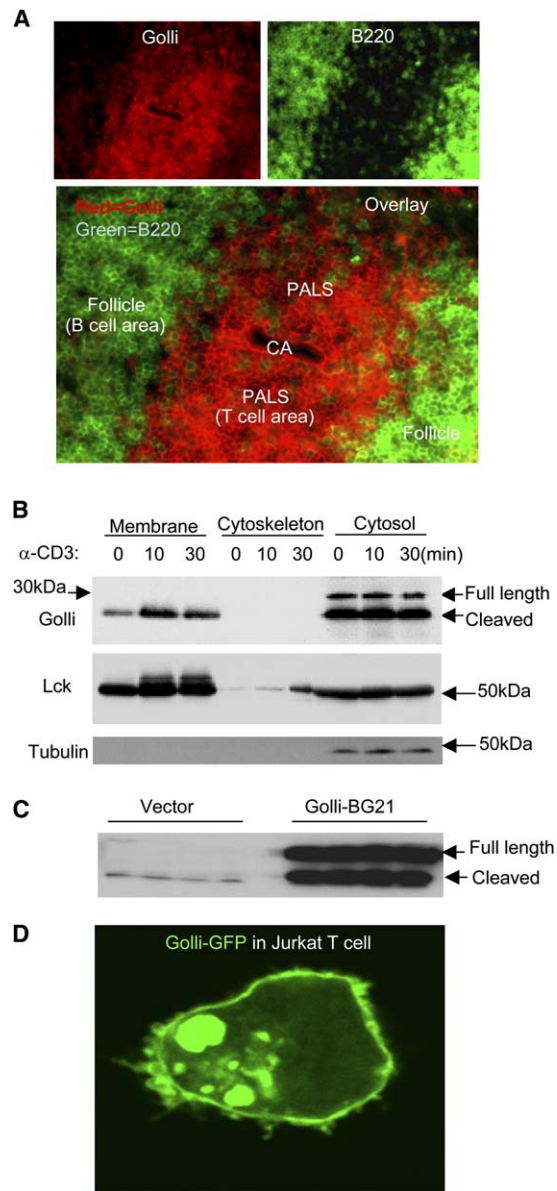

Figure 1. Preferential Expression of Golli Protein in T Cells in Mouse Spleen and Its Association with the Plasma Membrane after T Cell Activation

(A) Golli immunostaining in spleen tissues. Golli staining (green fluorescence) is shown in the upper-left panel; the same tissue section was also double stained with B220 (red fluorescence) (shown in the upper-right panel) to reveal B cell follicles. The lower panel represents the overlay image of golli and B200 staining. PALS, periarteriolar lymph sheath; CA, central arteriole.

(B) Fractionation assay. Primary T cells from lymph nodes were fractionated into cytosol, plasma membrane, and cytoskeleton fractions. Golli, Lck, and tubulin distribution was examined by immunoblot. The amount of proteins loaded in each lane is equivalent to that from 3×10^6 cells.

(C) Immunoblot showing intact and cleaved BG21 after transfection into Jurkat T cells. Cells were transfected with a control vector (pcDNA3.1) or a plasmid-containing cDNA sequence encoding golli BG21, and whole-cell lysates were separated by SDS-PAGE. Golli-specific antibody was used to detect immunoreactive bands.

(D) Membrane distribution of golli BG21-GFP in transfected Jurkat T cells. The confocal image shows a typical cell transfected with golli BG21-GFP. The data are representative of three independent determinations for each experiment.
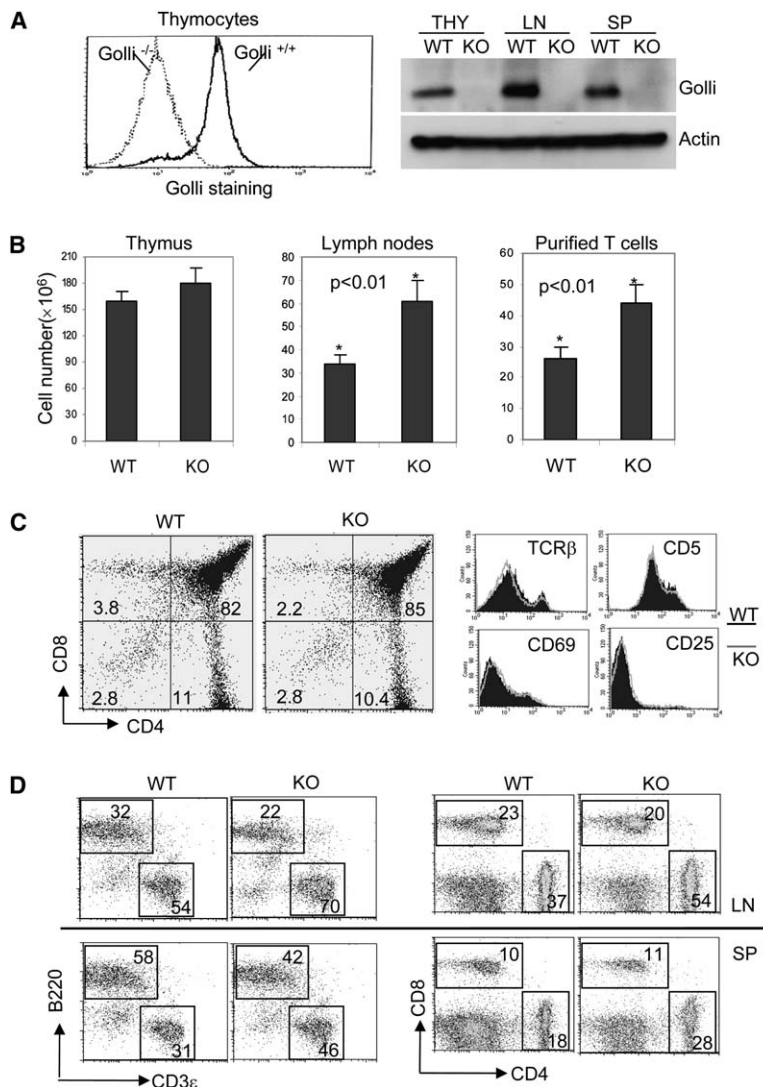
Figure 2. Normal Thymocyte Development, but Abnormal Accumulation of Peripheral T Cells, in Golli-Deficient Mice

(A) Flow cytometry assay of golli immunocytochemical staining in thymocytes (left panel) and immunoblot analysis of golli protein in the cell lysates of lymphoid cells (right panel) in golli WT and KO mice. THY, thymocytes; LN, lymph node cells; SP, splenocytes.

(B) Comparison of cell numbers in the lymphoid organs of golli WT and KO mice. Cells recovered from the following organs of each individual mouse were calculated after counting: thymus (∼4- to 6-week-old, left panel), pooled lymph nodes (cervical + axillary + inguinal lymph nodes, middle panel), and purified T cells (left panel) from spleen plus lymph nodes (12-week-old) after purification with T cell-enrichment columns. All data are expressed as the mean value ± SD (WT, n = 10; KO, n = 15; *p < 0.01, Student's t test).

(C) Flow cytometry assay of surface markers related to thymocyte development. The numbers in quadrants show the percentage of each thymocyte population defined by CD4 and CD8. The histograms show the expression of TCRβ, CD5, CD69, and CD25 in total thymocytes.

(D) Distribution of CD3⁺ versus B220⁺ cells and CD4⁺ versus CD8⁺ T cells in the lymph nodes (LN) and spleen (SP) of WT (WT, n = 5) and golli-deficient (KO, n = 5) mice. The numbers represent the percentage of designated cell populations, and the data represent five experiments.

genetic background of 129 and C57BL/6, and they are fertile and grossly normal.
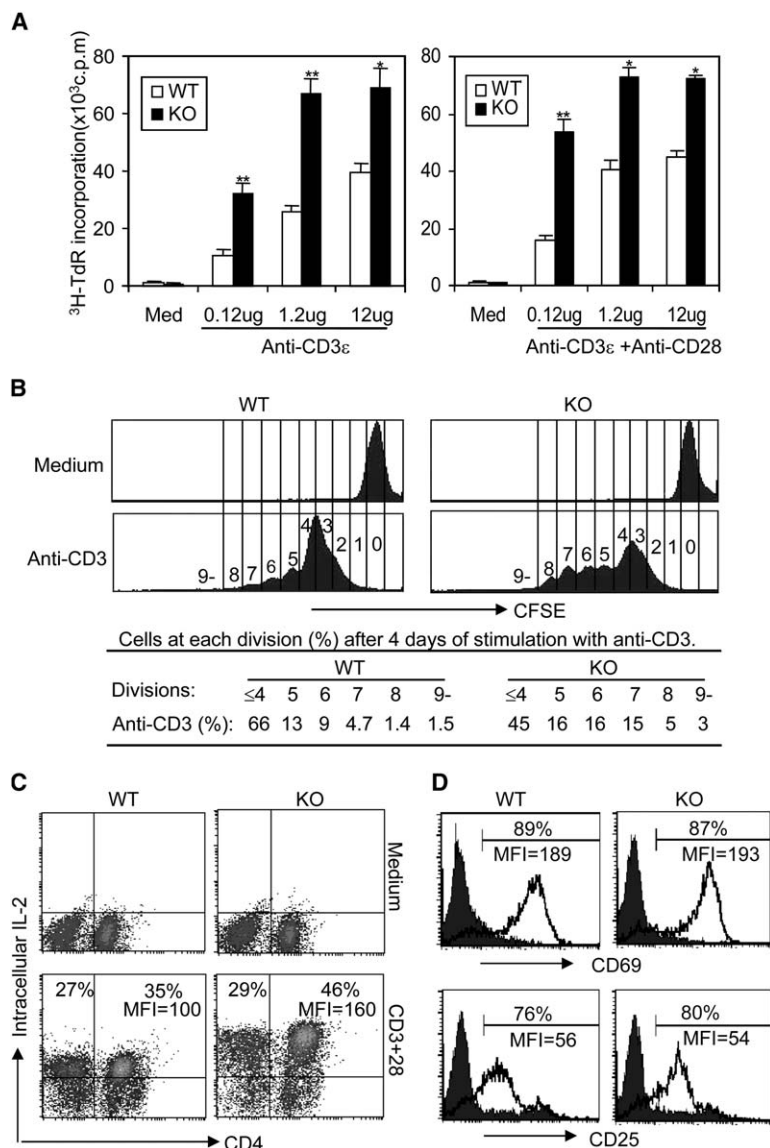
Examination of thymocyte development in golli-deficient mice revealed no alteration in the appearance and/or cellularity of the thymus, or in the total cell number of thymocytes (Figure 2B, left panel). Distribution of the major thymic cell populations, as assessed by the expression of CD4 and CD8 markers, was not altered (Figure 2C, left panels). Expression amounts of surface markers for developing thymocytes, such as TCRβ, CD5, CD69, and CD25, were also unaffected (Figure 2C, right panels). Thymocytes from golli-deficient and wild-type (WT) mice were equally sensitive to apoptosis induced by either anti-CD3 or dexamethasone (Figure S2). These data suggested that there were no defects in thymocyte development in golli-deficient mice.

Nonetheless, we regularly recovered at least twice as many cells from golli-deficient lymph nodes compared to controls (WT: 3.2 ± 0.2 × 10⁷; KO: 6.6 ± 0.3 × 10⁷; see Figure 2B, middle panel). This elevation appeared to be due to increased numbers of T cells because we recovered proportionately more T cells from golli-

deficient lymph node cells applied to T cell enrichment columns (Figure 2B, right panel). FACS analysis also showed an increased ratio of CD3⁺ T cells relative to the B220⁺ B cell population (WT: 1.6 ± 0.02, KO: 3.2 ± 0.03 in LN; WT: 0.5 ± 0.02, KO: 1.1 ± 0.04 in SP) and a biased ratio in the CD4⁺ versus CD8⁺ T cell populations (WT: 1.6 ± 0.02, KO: 2.8 ± 0.03 in LN; WT: 1.8 ± 0.02, KO: 2.6 ± 0.01 in SP) in golli-deficient lymph nodes (Figure 2D, upper panels) and spleens (Figure 2D, lower panels). These data indicated that golli deficiency caused an abnormal accumulation of T cells in the peripheral lymphoid organs.

Golli-Deficient T Cells Are Hyperproliferative

The biased T cell accumulation in the peripheral lymphoid organs of golli-deficient mice prompted us to examine the effect of golli deficiency on T cell proliferation. We isolated naive CD4⁺ T cells (CD44^low CD62L^hi) from pooled splenic and lymph node cells and incubated them with a range of concentrations of anti-CD3 in the absence or presence of a fixed concentration of anti-CD28. In both cases (Figure 3A), golli-deficient T cells

A

B

Cells at each division (%) after 4 days of stimulation with anti-CD3.

Divisions:	WT						KO					
	≤4	5	6	7	8	9-	≤4	5	6	7	8	9-
Anti-CD3 (%):	66	13	9	4.7	1.4	1.5	45	16	16	15	5	3

C

D

Figure 3. Hyperproliferation of Golli-Deficient T Cells

(A) Proliferation assay by thymidine incorporation. Purified, naive CD4+ T cells were stimulated with the indicated concentrations of anti-CD3ε in the absence (left panel) or presence (right panel) of a fixed concentration of anti-CD28 (5 μg/ml). Proliferation was measured by ^{3}H-thymidine incorporation after 72 hr. The data represent three independent experiments and are shown as the mean value of triplicate experiments ± SD (*p < 0.01, **p < 0.001, Student's t test).

(B) Proliferation analysis by CFSE labeling. CFSE-labeled, naive CD4+ T cells were stimulated with plate bound anti-CD3ε (10 μg/ml) and analyzed by flow cytometry after 4 days in culture. The numbers in the histograms indicate the cell divisions, and the table shows the percentage distributions of cells at each division. The data represent three independent experiments.

(C) Intracellular staining of IL-2 in primary T cells was assayed by flow cytometry. The percentage represents the IL-2-producing cells among CD4+ T cells; the number shows the staining intensity (MFI) of intracellular IL-2. The data are representative of three experiments.

(D) Comparable surface expression of CD69 and CD25. Purified CD4+ T cells from the lymph nodes of WT and KO mice were assayed by flow cytometry 16 hr after stimulation with 1 μg/ml plate bound anti-CD3ε plus 10 μg/ml soluble anti-CD28. Filled, unstimulated; open, stimulated with anit-CD3 + CD28. The data are representative of five experiments.

showed enhanced proliferation. This was especially evident at low doses of anti-CD3, suggesting that golli deficiency lowered the threshold for T cell activation. This observation was corroborated by labeling purified naive CD4+ T cells with carboxyfluorescein diacetate succinimidyl ester (CFSE), incubating the cells with anti-CD3 to promote proliferation, and then analyzing the cells by flow cytometry to directly measure the number of cell divisions. Golli-deficient naive CD4+ T cells divided substantially more rapidly than WT cells (Figure 3B), confirming the normal role of golli as an inhibitor of T cell activation.

Increased IL-2 Production in Golli-Deficient T Cells

IL-2 is an important growth factor for T cell proliferation, so we examined the amounts of this cytokine in golli-deficient T cells by FACS analysis. Flow cytometry (Figure 3C) indicated that golli-deficient CD4+ T cells produce more IL-2 upon stimulation with anti-CD3 + CD28, as reflected by an increase in both the percentage of IL-2-producing CD4+ T cells (i.e., 46% versus 35%), as well as their staining levels (mean fluorescence intensity [MFI] of 160 versus 100).

After TCR engagement, T cell proliferation may result from either increased IL-2 production and/or elevated amounts of high-affinity IL-2 receptor α chain (IL-2Rα, CD25) on the T cell surface (Smith, 1989). To address the possibility that golli deficiency might be influencing the expression of the CD25-containing, high-affinity IL-2 receptor in the T cell, we compared the expression of CD69 and CD25 on the cell surfaces of purified CD4+ T cells isolated from golli-deficient and control mice. After stimulation for 16 hr with anti-CD3 and anti-CD28, golli-deficient and WT cells showed similar upregulation of CD25 and CD69 on their cell surfaces (Figure 3D). These results excluded an effect of golli deficiency on selective expression of the CD25-containing, high-affinity IL-2 receptor, suggesting that one possibility for the enhanced proliferation in golli-deficient T cells was due to increased IL-2 production.

Intracellular Ca^{2+} and MAPK Activation in Golli-Deficient T Cells

T cell proliferation after TCR engagement requires a co-ordinated signaling cascade. To determine the underlying mechanism of how golli negatively regulates T cell activation, several signaling pathways were examined in the golli-deficient T cells. After anti-CD3 stimulation, no differences were observed in the total tyrosine phosphorylation profile of golli-deficient and control T cells (data not shown). Activation of the two members of the MAPK (mitogen activated protein kinase) pathway, ERK (extracellular receptor activated kinase) and JNK (Jun amino-terminal kinase), has been shown to closely correlate with T cell activation (Pages et al., 1999; Dong et al., 2002). We found no differences in ERK or JNK activation in golli-deficient versus control T cells, as measured by their phosphorylation after anti-CD3 stimulation (Figure 4A), indicating that the absence of golli has no effect on these signaling pathways. However, calcium influx upon anti-CD3 crosslinking was found to be greatly increased in naive golli-deficient CD4$^+$ T cells compared to control cells (Figure 4B), suggesting a relationship between golli action and calcium homeostasis in T cells.

Golli Negatively Regulates Store Depletion-Induced Ca^{2+} Influx in T Cells

Sustained elevation of intracellular Ca^{2+} concentrations ([Ca^{2+}]$_i$) is very important for T cell proliferation and differentiation (Feske et al., 2000, 2001). Two steps are known to contribute to elevated [Ca^{2+}]$_i$ upon TCR engagement. One involves Ca^{2+} release from ER stores, which is triggered by IP3 generated through hydrolysis of PIP2 by PLCγ1 (Berridge, 1993; Clapham, 1995). The second is a sustained influx of extracellular Ca^{2+} initiated by ER store depletion (Putney, 1990; Parekh and Penner, 1997; Putney and McKay, 1999; Putney et al., 2001; Venkatachalam et al., 2002). We found no difference in the phosphorylation (i.e., activation) of PLCγ1 (Figure 5A, left panel), and we found comparable amounts of IP3 production (Figure 5A, right panel) in golli-deficient and WT T cells upon anti-CD3 stimulation. These results suggested that the Ca^{2+} release from the ER stores might not be affected by golli deficiency. Direct confirmation of this was provided by calcium imaging experiments. When purified naive CD4$^+$ T cells were loaded with Fura-PE3(AM), and stimulated by anti-CD3 in the absence of extracellular [Ca^{2+}]$_{ex}$, a minor elevation in [Ca^{2+}]$_i$ (representing Ca^{2+} release from intracellular stores) was observed, and there was no significant difference of this Ca^{2+} release between golli-deficient and control T cells (Figure 5B, left panels). However, when the medium was supplemented with 2 mM [Ca^{2+}]$_{ex}$, a substantially high elevation in [Ca^{2+}]$_i$ (representing Ca^{2+} influx) occurred after anti-CD3 crosslinking, and there was a significantly enhanced Ca^{2+} influx in the golli-deficient T cells compared to controls (Figure 5B, left panels). The data indicated that the elevated [Ca^{2+}]$_i$ observed in stimulated golli-deficient T cells was a result of Ca^{2+} entry from outside the cells rather that Ca^{2+} release from intracellular ER stores.

This was examined further by using thapsigargin (TG) to deplete internal Ca^{2+} stores independently of signals from surface receptors (Thastrup et al., 1990; Parekh
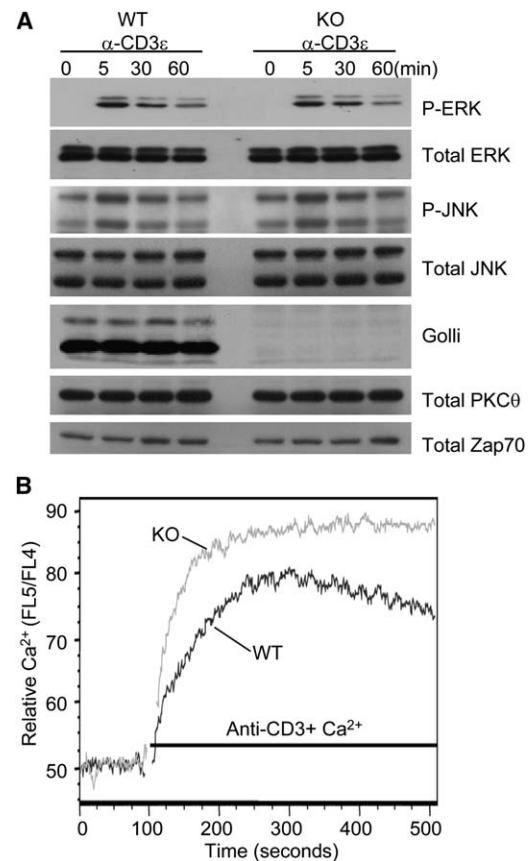

Figure 4. Normal Activation of ERK and JNK, but Enhanced Ca^{2+} Elevation, in Golli-Deficient T Cells

(A) Comparable ERK and JNK activation. Purified T cells were stimulated with soluble anti-CD3ε (2C11, 5 μg/ml); the phosphorylation of ERK (P-ERK) and JNK (P-JNK) was examined by immunoblot. The blots were sequentially blotted with PKCθ and ZAP70 to monitor the equal loading of the proteins.

(B) Ca^{2+} assay. Indo-1-loaded, naive T cells were stimulated by TCR crosslinking (anti-CD3 crosslinking) in normal medium containing calcium. The kinetic changes of Ca^{2+} influx were analyzed by flow cytometry. The data represent three experiments.

and Penner, 1997). TG acts by inhibiting the sarcoplasmic endoplasmic reticulum Ca^{2+} ATPase (SERCA), which pumps Ca^{2+} from the cytoplasm back to the ER stores. TG treatment in the absence of external Ca^{2+} induced comparable amounts of Ca^{2+} release from the internal stores in golli-deficient and WT T cells (Figure 5B, right panels). In contrast, greater Ca^{2+} entry was observed in golli-deficient versus WT T cells treated with TG in the presence of 2 mM [Ca^{2+}]$_{ex}$ (Figure 5B, right panels). These results were supported in a flow cytometric Ca^{2+} assay performed on Indo-1-loaded T cells (Figure S3). Thus, golli did not appear to act at the level of IP3-induced Ca^{2+} store release, but rather at the level of store depletion-induced Ca^{2+} entry into T cells at the plasma membrane, where it appeared to serve as a negative regulator.

Inreased CRAC Current in Golli-Deficient T Cells

In the T cell, Ca^{2+} influx is thought to result from activation of CRAC channels (calcium release-activated calcium channels), a subclass of SOCCs on the plasma
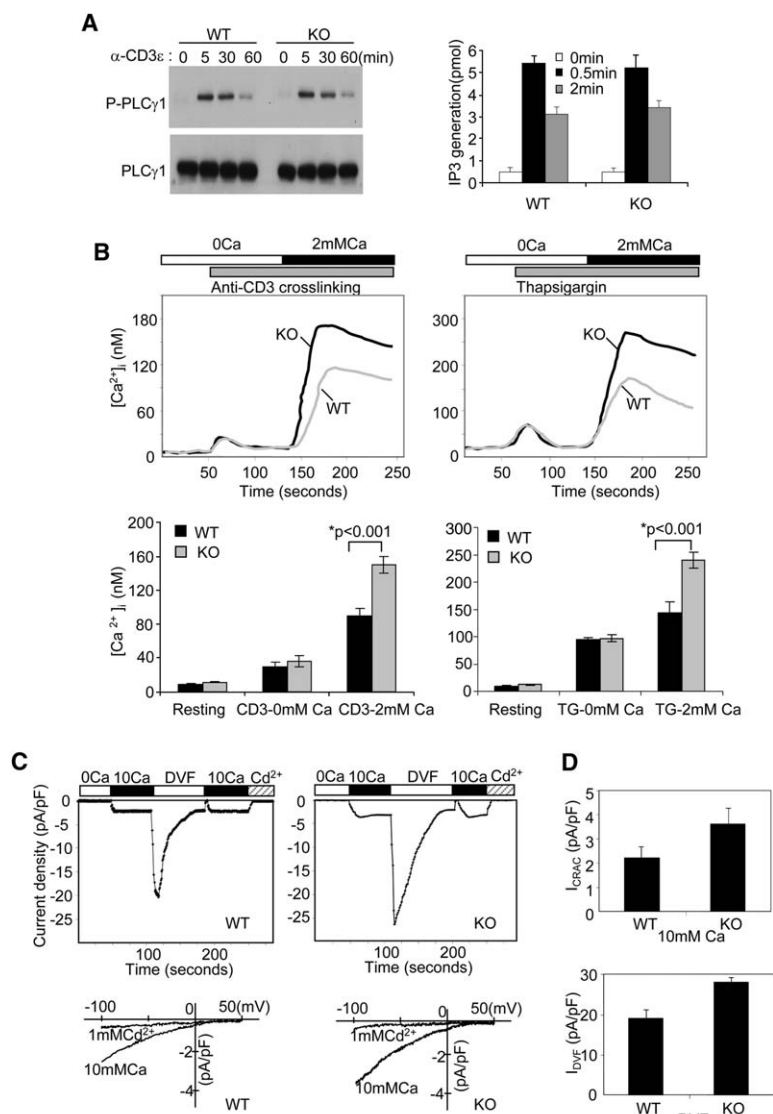
A

B

C

D

Figure 5. Enhanced Store Depletion-Induced Ca^{2+} Entry and I_{CRAC} in Golli-Deficient T Cells

(A) Detection of $PLC\gamma1$ activation and IP3 production. Phosphorylation of $PLC\gamma1$ (P-$PLC\gamma1$) was examined by immunoblot (left), and IP3 concentration was determined by radioimmunoassay (right) in primary T cells stimulated with anti-CD3 (5 μg/ml). The data represent three independent experiments and are shown as the mean value of triplicate determinations ± SD.

(B) Measurement of calcium release and influx. Intracellular Ca^{2+} release and influx were analyzed by calcium imaging in Fura-PE3-loaded T cells from golli WT and KO mice. For TCR stimulation, biotinylated anti-CD3 antibody (5 μg/ml, Biolegend San Diego) was crosslinked with streptavidin (5 μg/ml), as indicated by the absence of external Ca^{2+}, to measure intracellular Ca^{2+} release, followed by the addition of 2 mM Ca^{2+} to measure influx (top left). Ca^{2+} release and influx in response to TG (1 μM) treatment in T cells from golli WT and KO mice are shown in the top-right panel. The bottom histograms show the statistical summaries of the intracellular Ca^{2+} concentrations for golli WT (n = 30 cells) and KO T cells (n = 40 cells) in response to anti-CD3 crosslinking (bottom left) and TG treatment (bottom right). The data are shown as mean values ± SD (Student's t test, *p < 0.001).

(C) Patch clamp recording of the CRAC current. Time courses of I_{CRAC} show the response of WT (top left) and KO (top right) cells to store depletion induced by TG. Maximal current density was analyzed at −100 mV. The recording was performed sequentially under the following conditions: Ca^{2+}-free solution, readdition of 10 mM Ca^{2+} in the external solution, divalent ion-free solution (DVF), 10 mM Ca^{2+} in external solution, and 1 mM $CdCl_2$ in external solution. Leak-subtracted current-voltage relationships of fully developed I_{CRAC} currents in WT and KO T cells are shown in the bottom panels; these Ca^{2+} currents can be blocked by the addition of 1 mM $CdCl_2$ in the bath solution.

(D) Statistical summaries of the Ca^{2+} (I_{CRAC}, top panel) and Na^+ (DVF, bottom panel) current densities in WT and KO T cells. The data are summarized from five WT and six KO cells in an I_{CRAC} experiment and from four WT and five KO cells in a DVF experiment, respectively. They are shown as the mean value ± SD (Student's t test, p < 0.001).

membrane (Lewis, 2001). We compared CRAC current (I_{CRAC}) induced by store depletion in golli WT and KO T cells (Figure 5C). The store depletion was achieved by incubation of cells with 1 μM TG in Ca^{2+}-free external solution, and I_{CRAC} was measured by whole-cell recording after the subsequent addition of 10 mM external Ca^{2+}, a concentration that saturates the channel's conductance (Premack et al., 1994; Partiseti et al.,1994; Fanger et al., 1995). Figure 5C illustrates the time course of the inward I_{CRAC} development (Figure 5C, top panels) and the characteristic I-V relationship (Figure 5C, bottom panels) voltage ramps from −100 to +50 mV in a typical WT or KO T cell. Both WT and KO T cells generated the inward Ca^{2+} currents with the characteristics of CRAC currents. These currents showed an inward rectified current-voltage relationship without an obvious reversal potential that could be blocked by the addition

of cadmium (Cd^{2+}; Figure 5C, bottom panels). Removal of all external divalent cations (Ca^{2+} and Mg^{2+}) caused a large inward Na^+ current that subsequently declined slowly (Figure 5C, top panels). In golli-deficient T cells, both the inward I_{CRAC} (Figure 5D, top panel) and I_{DVF} (Figure 5D, bottom panel) were substantially enhanced in most of the observed cells. The enhancement of I_{CRAC} in golli-deficient T cells is consistent with the higher amplitude of Ca^{2+} influx measured by the calcium imaging and flow cytometry experiments described above. These data suggest that the high amount of Ca^{2+} influx in golli-deficient T cells is likely due to the increased CRAC channel activity.

Membrane Association of Golli

Because golli proteins are found constitutively associated with the plasma membrane of the T cells (as shown

in Figures 1B and 1D), we examined how this membrane association might affect Ca^{2+} influx in T cells. To disrupt the membrane association of golli, a myristoylation mutant of golli, i.e., golli BG21 (MYR), was generated through site-directed mutagenesis. In this construct, glycine at position 2 in WT golli BG21 (WT), which is the potential site for posttranslational myristoylation, was converted to an alanine. Jurkat cells were transfected with the WT- or MYR-BG21 tagged with GFP and were examined by confocal microscopy (Figure 6A). There was a clear association of the transfected WT-BG21-GFP with the plasma membrane in both xy-Z and xz-Y optical sections through the nuclei (Figure 6A, left panels), whereas the MYR-BG21-GFP was diffusely distributed throughout the cells, with no clear association with the membrane (Figure 6A, right panels). This was confirmed by biochemical studies (Figure 6B). A plasma membrane fraction (MEM) was isolated from the transfected Jurkat cells, and Lck was used as a marker to monitor the purity of this fraction. Although MYR- and WT-BG21 were equally detected by immunoblot in whole-cell lysates (WCL), the MYR-BG21 was absent from the plasma membrane (Figure 6B), suggesting that myristoylation is required for golli to be targeted to the membrane.

We next examined the effect of the loss of membrane association of BG21 on Ca^{2+} influx. Jurkat T cells were transfected with WT- or MYR-BG21, and store depletion-induced Ca^{2+} influx was measured after TG treatment. In the absence of $[Ca^{2+}]_{ex}$, Ca^{2+} release from internal stores by TG treatment was the same in WT-, MYR-BG21, and control empty vector-transfected cells (Figure 6C). After adding Ca^{2+} to the medium, however, Ca^{2+} influx in cells transfected with WT-BG21 was substantially reduced compared to the empty vector-transfected controls (Figure 6C). In MYR-BG21-transfected cells, inhibition observed by WT-BG21 was almost eliminated (Figure 6C), indicating that membrane association is essential for the inhibitory action of BG21 on store depletion-induced Ca^{2+} entry.

Golli-Deficient Mice Are Resistant to EAE
Since T cells are the central players in autoimmune disease, and golli plays a role in regulating T cell activation, we examined the potential role of golli in regulating the pathogenesis of an autoimmune disease such as EAE. Golli-deficient mice were tested for EAE induction by immunization with MOG. The results indicated that the golli-deficient mice were resistant to EAE induction, exhibiting both reduced incidence (Figure 7A) and severity (Figure 7B) of EAE. By day 25 postimmunization, all of the WT control mice had developed severe EAE. Only 20%–30% of the golli-deficient mice showed symptoms of EAE, and their symptoms were substantially milder than those of the WT animals (Figures 7A and 7B).

At first glance, these results might appear to be in apparent conflict with the hyperproliferative response of golli-deficient T cells. However, golli-deficient T cells respond to TCR engagement by enhancing Ca^{2+} influx above that of normal T cells. Elevated Ca^{2+} in the cytosol has been reported to induce T cell anergy in the adaptive immune response (Macian et al., 2002, 2004). Resistance of EAE induction in golli-deficient mice might reflect the fact that golli-deficient T cells preferentially dif-
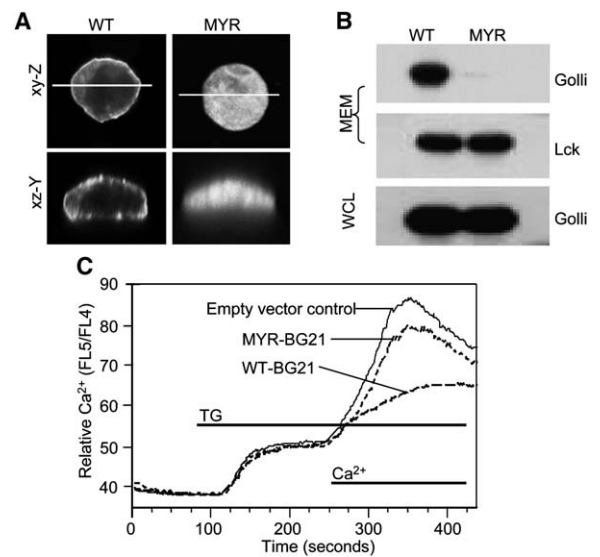

Figure 6. Membrane Association Is Required for Golli Protein to Inhibit the Store Depletion-Induced Ca^{2+} Influx

(A) Confocal microscope images of Jurkat T cells transfected with GFP-tagged golli WT- or MYR-BG21. The images in the xy-Z plane (top panels) were scanned through nuclei. The lines in xy-Z images indicated the scanning position of the xz-Y images (bottom panels) in the same cells. The cells shown are typical of cells in all five experiments.
(B) Examination by immunoblot of the transfected WT- and MYR-BG21 in fractionated cell lysates. MEM, plasma membrane fraction; WCL, whole-cell lysates.
(C) Analysis of store depletion-induced calcium influx by flow cytometry on Indo-1-loaded WT- or MYR-BG21-transfected Jurkat T cells. The data represent three independent experiments.

ferentiate into anergic cells during the adaptive immune response as a consequence of increased $[Ca^{2+}]_i$. To test this, MOG-specific T cell proliferation was examined in golli-deficient mice 12 days after immunization, when antigen-specific T cells have fully differentiated into effector cells. The MOG-specific T cells in the golli-deficient mice proliferated poorly compared to the WT controls (Figure 7C), indicating that golli-deficient T cells might be increasingly anergic relative to normal T cells.

Discussion

The function of golli-MBP expression in the immune system has not been defined. Because golli shares MBP epitopes with the classic MBPs, and is expressed in the developing thymus, some studies have been performed on its potential role as a myelin self-antigen to induce tolerance. However, studies with MBP1-11-specific TCR transgenic mice (Goverman et al., 1993; Lafaille et al., 1994) indicate that the presence of golli proteins in the thymus does not induce clonal deletion of the MBP1-11-specific T cells, although this classic MBP1-11 sequence is found within golli proteins. Our finding that T-lineage cells are the primary cell types expressing golli in the immune system (Feng et al., 2000, 2004) strongly suggests that rather than passively serving as a self-antigen to provide MBP epitopes in the immune system, golli may play a functional role in T cells. Supporting this notion, in vitro transfection of golli into
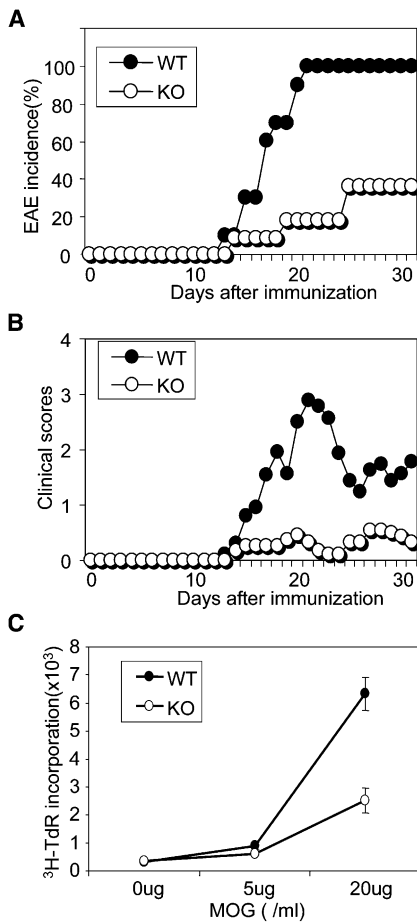
A

B

C

Figure 7. Resistance of EAE Induction in Golli-Deficient Mice

(A) Incidence of EAE induction by MOG immunization. The percentage of mice with EAE symptoms was plotted along with the days after immunization.

(B) Mean clinical scores of EAE symptoms in golli WT and KO mice. The experiment (A and B) was performed twice, and 40 mice (WT = 20 and KO = 20, respectively) were used each time.

(C) Proliferation assay of the MOG-specific immune response. Twelve days after immunization with MOG, purified CD4+ T cells from WT or KO draining lymph nodes were restimulated with MOG in the presence of irradiated syngeneic splenocytes as the antigen presenting cells. Proliferation was measured by ^{3}H-TdR incorporation. The data represent three independent experiments and are shown as the mean value of triplicate determinations ± SD.

Jurkat cells indicates that golli can inhibit T cell activation by TCR engagement (Feng et al., 2004). In the present study, we show that the ablation of golli in T cells results in hyperproliferation, indicating that golli negatively regulates T cell activation.

Despite the expression of golli in developing thymocytes, golli deficiency does not alter thymocyte development. The total cell numbers and the cellularity of CD4 and CD8 thymocytes from golli-deficient thymus are comparable to that in WT controls. Functionally, the golli-deficient thymocytes show equivalent sensitivity to induction of apoptosis by either anti-CD3 or dexamethasone. This is not too surprising, because many signaling molecules exhibit cell type-specific regulation. For example, PKCθ and Cbl-b are both expressed in thymocytes and peripheral T cells, but PKCθ- and Cbl-

b-deficient mice only show altered functions in peripheral T cell activation, whereas thymocyte development is quite normal (Sun et al., 2000; Bachmaier et al., 2000; Chiang et al., 2000). An alternative explanation for the lack of an effect of golli deficiency on thymocyte development might be that the expression levels of golli in DP thymocytes, the major cell population in thymus, are much lower than those in mature SP thymocytes (Feng et al., 2000), which are the counterparts of peripheral T cells. This higher level of expression of golli in the mature T cell might render the cell more sensitive to a loss of golli and result in a more prominent alteration of peripheral T cell function.

Although golli-deficient peripheral T cells are hyperproliferative upon stimulation in vitro, golli-deficient mice (in 129xC57BL/6 background) show only slightly enlarged lymph nodes, and they develop neither splenomegaly nor spontaneous autoimmune disease, suggesting that golli-deficient T cells do not undergo unrestrained proliferation in vivo. In this regard, golli is different from other negative regulators of T cell signaling pathways. For example, the hyperactivation of Cbl-b-deficient T cells leads to the development of spontaneous autoimmune lymphocyte infiltration in multiple organs in these mice (Bachmaier et al., 2000), as well as increased sensitivity to EAE induction (Chiang et al., 2000). In golli-deficient mice, the consequence of hyperactivation of T cells is not hypersensitivity to EAE induction, but, rather, resistance to MOG-induced EAE. In this regard, golli-deficient mice are quite similar to $Drak2^{-/-}$ mice, which have been shown recently to exhibit hyperproliferation of T cells in vitro but are resistant to EAE induction in vivo (McGargill et al., 2004). Resistance to EAE induction in golli-deficient mice seems to be at odds with the hyperproliferative response of golli-deficient T cells. However, unlike other negative regulators of T cell activation, such as Cbl-b and DGK, which apparently act on the kinase arm of TCR signaling (Bachmaier et al., 2000; Chiang et al., 2000; Zhong et al., 2003), golli negatively regulates TCR signaling by inhibiting external calcium uptake through the plasma membrane of the T cell. We found that Ca^{2+} uptake in golli-deficient T cells substantially increased upon TCR crosslinking, and no differences were observed in the activation of ERK or JNK. While sustained elevation of calcium influx upon TCR engagement is required for T cell proliferative clonal expansion in the initial immune response, elevated Ca^{2+} in the cytosol also induces T cell anergy in the subsequent adaptive immune response (Macian et al., 2004). In a study by Rao's group (Macian et al., 2002), pretreatment of T cells with ionomycin resulted in their unresponsiveness (anergy) to subsequent restimulation. Our examination of the MOG-specific adaptive immune response revealed that golli-deficient T cells show an anergic phenotype by exhibiting poor proliferation, suggesting that golli deficiency uncouples the hyperactivation of T cells to the hypersensitivity of autoimmune disease. The resistance of EAE induction in golli-deficient mice may reflect a dual function of golli in regulating T cell clonal expansion and in subsequent effector cell differentiation. It may suggest that although the golli-deficient T cell is hyperproliferative in the initial clonal expansion, it preferentially differentiates into an anergic phenotype in the

adaptive immune response due to enhanced elevation of Ca^{2+} in the cytosol. This speculation needs to be further defined.

In the T cell, Ca^{2+} influx is thought to be the result of activated CRAC channels, a subclass of SOCCs on the plasma membrane (Lewis, 2001; Feske et al., 2005). These channels can be activated by depletion of intracellular stores with TG, an ER pump blocker. In golli-deficient T cells, the enhanced Ca^{2+} influx induced by TCR engagements can also be observed by TG treatment, suggesting that golli might regulate downstream signals after internal Ca^{2+} store depletion-induced activation of CRAC channels. Our patch clamp observations demonstrated enhanced I_{CRAC} in individual golli-deficient T cells. However, it is not yet clear whether this is due to a direct effect of golli on an existing CRAC channel, or whether golli deficiency causes an upregulation of I_{CRAC} channel expression or its activation pathway.

CRAC channel activity is fine tuned by both positive and negative regulation. The recent finding with STIM1 supports this notion. STIM1 is a ubiquitously expressed membrane protein that has been found to regulate CRAC channel function in a positive fashion (Roos et al., 2005; Liou et al., 2005). STIM1 has been proven to serve as a Ca^{2+} sensor that activates CRAC channels and migrates from the Ca^{2+} stores to the plasma membrane (Zhang et al., 2005). The molecular identities of CRAC channels remain unclear. The best candidates for CRAC channels so far are members of the transit receptor potential (TRP) superfamily of signal transduction-gated ion channels (Montell et al., 2002; Yue et al., 2001; Cui et al., 2002). Interestingly, many members of the TRP family show spontaneous channel activity (Dietrich et al., 2003), suggesting that they need certain negative regulators to maintain them in a closed status in order to prevent unrestrained Ca^{2+} influx. The small molecular weight of golli (only ∼25–30 kDa) and its association with the plasma membrane make it a good candidate for such a negative regulator of CRAC activation pathway.

We observed that in primary T cells golli proteins have undergone extensive cleavage. A substantial portion of this "cleaved" golli protein is constitutively associated with the plasma membrane, and this association increased upon TCR engagement, suggesting that the inhibitory action of golli might be at the plasma membrane. Our mutagenesis study provided further evidence for this, since mutation of the myristoylation site on golli disrupted its association with the plasma membrane and reversed its inhibitory function on Ca^{2+} influx in Jurkat T cells, indicating that the membrane association of golli protein is essential for its inhibitory action.

The finding that golli can negatively regulate store depletion-induced Ca^{2+} influx in T cells defines a unique immunological function of golli protein to regulate T cell activation through modulation of Ca^{2+} homeostasis.

Experimental Procedures

Immunohistochemistry
Spleens removed from 2-month-old C57BL/B6 mice (all animal procedures used in this study have been approved by the UCLA Animal Research Committee) were fixed overnight at 4°C in 4% paraformaldehyde and then embedded in OCT cryostat medium. Double immunostaining of golli (affinity-purified polyclonal antibody from rabbit) and B220 (rat monoclonal antibody, Pharmingen) was performed on 5 μm cryostat tissue sections. After blocking with 1% BSA in PBS for 30 min, the sections were incubated with primary antibody cocktails (golli antibody 1:1000 + B220 antibody 1:200) for 1 hr at room temperature. After three washes with 0.05% Tween-20 in PBS, the sections were incubated for 45 min with fluorescence-labeled secondary antibody cocktails (anti-rabbit-Texas red 1:400 + anti-rat-FITC 1:200). After washes, the sections were mounted in Vectashield (Vector Lab). Fluorescence images were analyzed by using Leica DM RXA fluorescence microscope.

Subcellular Fractionation
Single cell suspensions from lymph nodes and spleens were passed through T cell enrichment columns to obtain the purified primary T cells. Primary T cells (5 × 10⁷) were suspended in 160 μl hypotonic buffer (42 mM KCl, 5 mM MgCl₂, 10 mM HEPES buffer [pH 7.4], with 2.5 μg/ml of aprotonin and leupeptin), incubated on ice for 15 min, passed through a 27 gauge needle 15 times, and centrifuged at 1,800 rpm at 4°C for 10 min to remove nuclei and unbroken cells. A 160 μl aliquot of supernatant was centrifuged for 40 min at 14,000 rpm in an Eppendorf centrifuge at 4°C. The resulting supernatant was designated as "cytosol." After a 200 μl wash with hypotonic buffer, the pellet was suspended in 160 μl lysis buffer (1% NP-40, 150 mM NaCl, 5 mM EDTA, 5 mM NaPP, 1 mM NaVO₄, 20 mM Tris-HCl buffer [pH 7.5], with 2.5 μg/ml of aprotonin and leupeptin), incubated on ice for 15 min, and centrifuged at 14,000 rpm for 40 min. The supernatant was designated as the "plasma membrane fraction." The pellet, after washing once with hypotonic buffer, was dissolved in 1% SDS and was designated the "cytoskeleton" fraction. For the immunoblot shown in Figure 1B, 10 μl aliquots (equivalent to ∼3 × 10⁶ cells) of proteins from cytosol, plasma membrane, and cytoskeleton fractions were run on a 10% SDS-PAGE gel.

Flow Cytometry
Single cell suspensions of thymi, lymph nodes, and spleen from golli KO and WT mice were stained with FITC-, PE-, Cychrome-, or APC-conjugated antibodies, including CD25, CD3ε, CD4, CD44, CD5, CD62L, CD69, CD8, and B220 (from Pharmingen). All samples were analyzed by FACS caliber (Becton Dickinson).

Proliferation and Cytokine Detection
The proliferation of MACs-purified naive CD44^low CD62L^hi CD4⁺ T cells was measured by ³H-thymidine incorporation and by CFSE labeling. The cells were stimulated with anti-CD3ε (clone 2C11, hamster IgG) and anti-CD28 (clone 37.51, Pharmingen). IL-2 production was measured by flow cytometry upon intracellular staining. Briefly, after stimulation with anti-CD3 + CD28, the cells were incubated with brefeldin A (10 μg/ml, Sigma) for an additional 6 hr to prevent the release of the cytokine from the cytoplasm. The IL-2 levels were determined by intracellular staining for IL-2 in the fixed cells.

IP3 Detection
Cells (4 × 10⁶) were stimulated with anti-CD3 (2C11, 5 μg/ml) at 37°C for the indicated time. IP3 levels were analyzed with the BioTrack IP3 radio immunoassay system (Amersham Biotech).

Calcium Assay by Flow Cytometry
Purified naive T cells or Jukat T cells (1 × 10⁷) were loaded with Indo-1 (2 μg/ml, Molecular Probe) by incubation for 45 min at 37°C in the presence of probenecid (4 mM) in cell loading medium (HBSS supplemented with 1 mM CaCl₂, 1 mM MgCl₂ and 0.5% BSA). Loaded cells were washed four times with Ca^{2+}- and Mg^{2+}-free-HBSS (containing 0.5% BSA). For anti-CD3 crosslinking, the primary T cells were incubated with 5 μg/ml anti-CD3ε (2C11) on ice for 20 min. The antibody bound cells were then washed, and a baseline level of Ca^{2+} was determined by flow cytometry at 37°C. Crosslinking was performed by adding prewarmed HBSS (Ca^{2+}- and Mg^{2+}-free) containing 20 μg/ml anti-hamster IgG with or without 2 mM CaCl₂. Intracellular Ca^{2+} concentration was monitored by using the calcium template on BD FACS LSR. The final data were analyzed by Flowjo Flow Cytometric Data Analysis Software. For the store depletion study, the Indo-1-loaded cells were treated with either ionomycin (100 ng/ml) or thapsigargin (1 μM, Sigma).

Calcium Imaging

Purified naive T cells from lymph nodes were loaded with 4 μM Fura-PE3 (AM) (Teflabs, Austin, TX) plus 0.08% Pluronic F-127 (Molecular Probes, Eugene, OR), then washed four times in RPMI 1640 for 45 min at 37°C. The loaded cells were then seeded on coverslips coated with poly-D-lysine for 30 min on ice. Ca^{2+} imaging was performed as described previously (Jacobs et al., 2005) with an Olympus epifluorescence microscope and image analysis software. The fluorescence of Fura-2 was excited alternatively at wavelengths of 357 and 380 nm by means of a high-speed wavelength-switching device.

Electrophysiology

Patch clamp experiments were done at room temperature in the whole-cell configuration as described previously (Cui et al., 2002). The cells were purified by the $CD4^+CD62L^+$ T Cell Isolation Kit (Miltenyi Biotech) with a purity >98%. These cells were stimulated for 24 hr with anti-CD3 (2 μg/ml) + anti-CD28 (2 μg/ml) to increase the size of the cells to facilitate patching. The diameter of these cells was ~17–20 μm with a capacitance of ~9–12 pF. There is no difference in size between WT and KO T cells. The Ca^{2+}-free external solution contained: 145 mM NaCl, 10 mM CsCl, 3 mM $MgCl_2$, 10 mM glucose, and 10 mM HEPES (pH 7.4; osmolality, 320 mM). Complete divalent-free (DVF) solution contained 115 mM NaCl, 10 mM HEPES (pH 7.4), 10 mM sodium EDTA, and 10 mM glucose. Ca^{2+}-containing external solution was prepared by the addition of 10 mM $CaCl_2$ to the Ca^{2+}-free external solution. Internal pipette solution contained: 140 mM Cs-aspartate, 2 mM Mg-ATP, 1 mM $MgCl_2$, 10 mM BAPTA, and 10 mM Cs-HEPES (pH 7.2; osmolality, 290 mM). The membrane potential was held at 0 mV. Voltage ramps were generated from −100 mV to 50 mV and lasted 300 ms.

Induction and Evaluation of EAE

Golli WT and KO mice (8–12 week of age) were immunized with 100 μg MOG in emulsified CFA (IFA supplemented with 5 mg/ml *Mycobacterium tuberculosis*) and injected intravenously on days 0 and 2 with 200 ng pertussis toxin. Clinical assessment of EAE was performed daily as the following: 0, no disease; 1, tail weakness; 2, hind limb weakness or partial paralysis; 3, complete hind limb paralysis; 4, fore limb weakness or paralysis; 5, moribund state or death.

Supplemental Data

Supplemental Data include Figures S1–S3 and are available at http://www.immunity.com/cgi/content/full/24/6/717/DC1/.

References

Bachmaier, K., Krawczyk, C., Kozieradzki, I., Kong, Y.Y., Sasaki, T., Oliveira-dos-Santos, A., Mariathasan, S., Bouchard, D., Wakeham, A., Itie, A., et al. (2000). Negative regulation of lymphocyte activation and autoimmunity by the molecular adaptor Cbl-b. Nature *403*, 211–216.

Berridge, M.J. (1993). Inositol trisphosphate and calcium signaling. Nature *361*, 315–325.

Campagnoni, A.T., and Skoff, R.P. (2001). The pathobiology of myelin mutants reveals novel biological functions of the MBP and PLP genes. Brain Pathol. *11*, 74–91.

Campagnoni, A.T., Pribyl, T.M., Campagnoni, C.W., Kampf, K., Amur-Umarjee, S., Landry, C.F., Handley, V.W., Newman, S.L., Garbay, B., and Kitamura, K. (1993). Structure and developmental regulation of Golli-mbp, a 105-kilobase gene that encompasses the myelin basic protein gene and is expressed in cells in the oligodendrocyte lineage in the brain. J. Biol. Chem. *268*, 4930–4938.

Chiang, Y.J., Kole, H.K., Brown, K., Naramura, M., Fukuhara, S., Hu, R.J., Jang, I.K., Gutkind, J.S., Shevach, E., and Gu, H. (2000). Cbl-b regulates the CD28 dependence of T-cell activation. Nature *403*, 216–220.

Clapham, D.E. (1995). Calcium signaling. Cell *80*, 259–268.

Cui, J., Bian, J.S., Kagan, A., and McDonald, T.V. (2002). CaT1 contributes to the stores-operated calcium current in Jurkat T-lymphocytes. J. Biochem. (Tokyo) *277*, 47175–47183.

Dietrich, A., Mederos y Schnitzler, M., Emmel, J., Kalwa, H., Hofmann, T., and Gudermann, T. (2003). N-linked protein glycosylation is a major determinant for basal TRPC3 and TRPC6 channel activity. J. Biochem. (Tokyo) *278*, 47842–47852.

Dong, C., Davis, R.G., and Flavell, R.A. (2002). MAP kinases in the immune response. Annu. Rev. Immunol. *20*, 55–72.

Fanger, C.M., Hoth, M., Crabtree, G.R., and Lewis, R.S. (1995). Characterization of T cell mutants with defects in capacitative calcium entry: genetic evidence for the physiological roles of CRAC channels. J. Cell Biol. *131*, 655–667.

Feng, J.M., Givogri, I.M., Bongarzone, E.R., Campagnoni, C., Jacobs, E., Handley, V.W., Schonmann, V., and Campagnoni, A.T. (2000). Thymocytes express the golli products of the myelin basic protein gene and levels of expression are stage dependent. J. Immunol. *165*, 5443–5450.

Feng, J.M., Fernandes, A.O., Campagnoni, C.W., Hu, Y.H., and Campagnoni, A.T. (2004). The golli-myelin basic protein negatively regulates signal transduction in T lymphocytes. J. Neuroimmunol. *152*, 57–66.

Feske, S., Draeger, R., Peter, H.H., Eichmann, K., and Rao, A. (2000). The duration of nuclear residence of NFAT determines the pattern of cytokine expression in human SCID T cells. J. Immunol. *165*, 297–305.

Feske, S., Giltnane, J., Dolmetsch, R., Staudt, L.M., and Rao, A. (2001). Gene regulation mediated by calcium signals in T lymphocyte. Nat. Immunol. *2*, 316–324.

Feske, S., Okamura, H., Hogan, P.G., and Rao, A. (2003). Ca^{2+}/calcineurin signaling in cells of the immune system. Biochem. Biophys. Res. Commun. *311*, 1117–1132.

Feske, S., Prakriya, M., Rao, A., and Lewis, R.S. (2005). A severe defect in CRAC Ca^{2+} channel activation and altered K^+ channel gating in T cells from immunodeficient patients. J. Exp. Med. *202*, 651–662.

Goverman, J., Woods, A., Larson, L., Weiner, L.P., Hood, L., and Zaller, D.M. (1993). Transgenic mice that express a myelin basic protein-specific T cell receptor develop spontaneous autoimmunity. Cell *72*, 551–560.

Jacobs, E.C., Pribyl, T.M., Feng, J.M., Kampf, K., Spreuer, V., Campagnoni, C., Colwell, C.S., Reyes, S.D., Martin, M., Handley, V., et al. (2005). Region-specific myelin pathology in mice lacking the golli products of the myelin basic protein gene. J. Neurosci. *25*, 7004–7013.

Lafaille, J.J., Nagashima, K., Katsugi, M., and Tonegawa, S. (1994). High incidence of spontaneous autoimmune encephalomyelitis in immunodeficient anti-myelin basic protein T cell receptor transgenic mice. Cell *78*, 399–408.

Landry, C.F., Ellison, J.A., Pribyl, T.M., Campagnoni, C., Kampf, K., and Campagnoni, A.T. (1996). Myelin basic protein gene expression in neurons: developmental and regional changes in protein targeting within neuronal nuclei, cell bodies, and processes. J. Neurosci. *16*, 2452–2462.

Lewis, R.S. (2001). Calcium signaling mechanisms in T lymphocytes. Annu. Rev. Immunol. *19*, 497–521.

Liou, J., Kim, M.L., Heo, W.D., Jones, J.T., Myers, J.W., Ferrell, J.E., Jr., and Meyer, T. (2005). STIM is a Ca^{2+} sensor essential for Ca^{2+}-store-depletion-triggered Ca^{2+} influx. Curr. Biol. *15*, 1235–1241.

Macian, F., Garcia-Cozar, F., Im, S.H., Horton, H.F., Byrne, M.C., and Rao, A. (2002). Transcriptional mechanisms underlying lymphocyte tolerance. Cell *109*, 719–731.

Macian, F., Im, S.H., Garcia-Cozar, F.J., and Rao, A. (2004). T-cell anergy. Curr. Opin. Immunol. *16*, 209–216.

McGargill, M.A., Wen, B.G., Walsh, C.M., and Hedrick, S.M. (2004). A deficiency in Drak2 results in a T cell hypersensitivity and an unexpected resistance to autoimmunity. Immunity *21*, 781–791.

Montell, C., Birnbaumer, L., and Flockerzi, V. (2002). The TRP channels, a remarkably functional family. Cell *108*, 595–598.

Pages, G., Guerin, S., Grall, D., Bonino, F., Smith, A., Anjuere, F., Auberger, P., and Pouyssegur, J. (1999). Defective thymocyte maturation in p44 MAP kinase (Erk 1) knockout mice. Science *286*, 1374–1377.

Parekh, A.B., and Penner, R. (1997). Store depletion and calcium influx. Physiol. Rev. *77*, 901–930.

Partiseti, M., Deist, F.L., Hivroz, C., Fischer, A., Korn, H., and Choquet, D. (1994). The calcium current activated by T cell receptor and store depletion in human lymphocytes is absence in a primary immunodeficiency. J. Biochem. (Tokyo) *269*, 32327–32335.

Premack, B.A., McDonald, T.V., and Gardner, P. (1994). Activation of Ca^{2+} current in Jurkat T cells following the depletion of Ca^{2+} stores by microsomal Ca$^{(2+)}$-ATPase inhibitors. J. Immunol. *152*, 5226–5240.

Putney, J.W. (1990). Capacitative calcium entry revisited. Cell Calcium *11*, 611–624.

Putney, J.W., and McKay, R.R. (1999). Capacitative calcium entry channels. Bioessays *21*, 38–46.

Putney, J.W., Broad, L.M., Braun, F.J., Lievremont, J.P., and Bird, G.S. (2001). Mechanisms of capacitative calcium entry. J. Cell Sci. *114*, 2223–2229.

Roos, J., DiGregorio, P.J., Yeromin, A.V., Ohlsen, K., Lioudyno, M., Zhang, S., Safrina, O., Kozak, J.A., Wagner, S.L., Cahalan, M.D., et al. (2005). STIM1, an essential and conserved component of store-operated Ca^{2+} channel function. J. Cell Biol. *169*, 435–445.

Smith, K.A. (1989). The interleukin 2 receptor. Annu. Rev. Cell Biol. *5*, 397–425.

Sun, Z., Arendt, C.W., Ellmeier, W., Schaeffer, E.M., Sunshine, M.J., Gandhi, L., Annes, J., Petrzilka, D., Kupfer, A., Schwartzberg, P.L., and Littman, D.R. (2000). PKC-θ is required for TCR-induced NF-κB activation in mature but not immature T lymphocytes. Nature *404*, 402–407.

Thastrup, O., Cullen, P.J., Drobak, B.K., Hanley, M.R., and Dawson, A.P. (1990). Thapsigargin, a tumor promoter, discharges intracellular Ca^{2+} stores by specific inhibition of the endoplasmic reticulum Ca$^{2(+)}$-ATPase. Proc. Natl. Acad. Sci. USA. *87*, 2466–2470.

Venkatachalam, K., van Rossum, D.B., Patterson, R.L., Ma, H.T., and Gill, D.L. (2002). The cellular and molecular basis of store-operated calcium entry. Nat. Cell Biol. *4*, E263–E272.

Voskuhl, R.R., Pribyl, T.M., Kampf, K., Handley, V., Liu, H.B., Feng, J., Campagnoni, C.W., Soldan, S.S., Messing, A., and Campagnoni, A.T. (2003). Experimental autoimmune encephalomyelitis relapses are reduced in heterozygous golli MBP knockout mice. J. Neuroimmunol. *139*, 44–50.

Yue, L., Peng, J.B., Hediger, M.A., and Clapham, D.E. (2001). CaT1 manifests the pore properties of the calcium-release-activated calcium channel. Nature *410*, 705–709.

Zhang, S.L., Yu, Y., Roos, J., Kozak, J.A., Deerinck, T.J., Ellisman, M.H., Stauderman, K.A., and Cahalan, M.D. (2005). STIM1 is a Ca^{2+} sensor that activates CRAC channels and migrates from the Ca^{2+} store to the plasma membrane. Nature *437*, 902–905.

Zhong, X.P., Hainey, E.A., Olenchock, B.A., Jordan, M.S., Maltzman, J.S., Nichols, K.E., Shen, H., and Koretzky, G.A. (2003). Enhanced T cell responses due to diacylglycerol kinase zeta deficiency. Nat. Immunol. *4*, 882–890.